

1 **Species composition determines bioplastics production in photosynthetic**
2 **microbiomes: strategy to enrich cyanobacteria PHB-producers**

3 Beatriz Altamira-Algarra^a, Artai Lage^a, Joan García^b, Eva Gonzalez-Flo^{a*}

^aGEMMA-Group of Environmental Engineering and Microbiology. Department of Civil and Environmental Engineering. Escola d'Enginyeria de Barcelona Est (EEBE). Universitat Politècnica de Catalunya-BarcelonaTech. Av. Eduard Maristany 16. Building C5.1. E-08019 Barcelona. Spain

^bGEMMA-Group of Environmental Engineering and Microbiology. Department of Civil and Environmental Engineering. Universitat Politècnica de Catalunya-BarcelonaTech. c/ Jordi Girona 1-3. Building D1. E-08034 Barcelona. Spain

* Corresponding author. GEMMA-Group of Environmental Engineering and Microbiology. Department of Civil and Environmental Engineering. Escola d'Enginyeria de Barcelona Est (EEBE). Universitat Politècnica de Catalunya-BarcelonaTech. Av. Eduard Maristany 16. Building C5.1. E-08019 Barcelona. Spain

4 E-mail address: eva.gonzalez.flo@upc.edu

5

6

7 **Abstract**

8 The aim of this study was to set the operating mode in regards to nutrients, temperature
9 and light to use as a strategy to enrich a microbiome rich in cyanobacteria in
10 polyhydroxybutyrate (PHB)-producers in order to enhance this biopolymer production.
11 Alternate growth and accumulation phases were conducted for 179 days in a 3 L
12 photobioreactor. Although, presence of green microalgae potentially reduced PHB
13 production, the microbiome produced up to 22 % dry cell weight (dcw) PHB. Results
14 suggested that this methodology could be applied to a robust microbiome rich in
15 cyanobacteria to boost PHB production.

16

17 **Keywords**

18 Polyhydroxyalkanoate

19 Microbiome

20 Biopolymer production

21

22 **Funding**

23 This research has received funding from the European Union's Horizon 2020 research
24 and innovation programme under the grant agreement No 101000733 (project
25 PROMICON). B. Altamira-Algarra thanks the Agency for Management of University
26 and Research (AGAUR) for her grant [FIAGAUR_2021]. E. Gonzalez-Flo would like
27 to thank the European Union-Next Generation EU, Ministry of Universities and
28 Recovery, Transformation and Resilience Plan for her research grant [2021UPF-MS-
29 12].

30

31 **1. Introduction**

32 Polyhydroxybutyrate (PHB) is a biopolymer synthesized by numerous bacterial species
33 as intracellular carbon and energy storage being fully biodegradable into CO₂ and H₂O
34 (Jendrossek and Handrick, 2002). Due to their physicochemical properties, PHB can be
35 used in different fields, such as in packaging or medicine (Manikandan et al., 2020;
36 Mohammadalipour et al., 2023). Industrial PHB production is nowadays based
37 exclusively on “pure” microbial cultures, which raises production expenses and makes
38 it difficult for PHB to be price competitive with traditional plastics (Tan et al., 2021).

39 Use of microbial “mixed” cultures (microbiomes) for PHB production has the potential
40 to comparatively reduce operational costs of pure cultures since they could be operated
41 in open systems not requiring sterilization, and utilize cheap by-products and waste
42 streams as feed (Fradinho et al., 2013a; Mohamad Fauzi et al., 2019; Reis et al., 2011).
43 This approach would engage the integration of the biopolymer production process
44 within the circular economy concept. To increase biopolymer production in
45 microbiomes two complementary strategies can be followed: (i) optimizing the culture
46 to enhance the presence of PHB-producers and (ii) modifying operating parameters with
47 an effect on PHB metabolic routes and subsequent synthesis. The called feast and
48 famine (FF) strategy has been successfully applied to enrich cultures in PHB-storing
49 organisms (Oliveira et al., 2017; Sagastume et al., 2017; Sruamsiri et al., 2020). FF
50 regime consists in a transient period of carbon source availability in which
51 microorganisms store PHB (feast phase). Followed by a prolonged period without carbon
52 addition (famine phase), where microorganisms use the stored biopolymer as an internal
53 carbon source. Repeated FF cycles create a selection pressure favorable for
54 microorganisms with the capacity to store PHB. Productivities up to 90 % dry cell
55 weight (%dcw) of PHB have been produced by heterotrophic microbiomes at laboratory
56 scale, which is comparable to those obtained by pure cultures (Johnson et al., 2009;
57 Serafim et al., 2004). However, until now, most of the experiments on PHB production
58 using FF have been performed by heterotrophic microorganisms, like activated sludge
59 using volatile fatty acids as substrate (Crognale et al., 2022; Estévez-Alonso et al.,
60 2022; Johnson et al., 2009; Serafim et al., 2004), while there is a wide diversity of
61 bacterial species that can produce this biopolymer and numerous operation conditions to
62 be tested.

63 Photosynthetic microorganisms, such as cyanobacteria, are also able to produce PHB.
64 Although production rates are lower than those obtained by heterotrophic bacteria
65 (Monshupanee and Incharoensakdi, 2014; Rueda et al., 2020a; Sharma and Mallick,
66 2005a), the interest of using a photosynthetic culture is the feasibility of using CO₂ and
67 sunlight for biomass growth and biopolymer synthesis (Rueda et al., 2020a). Laboratory
68 research on PHB production by cyanobacteria has been done using monocultures of, for
69 example, *Nostoc* sp., *Synechocystis* sp. and *Synechococcus* sp. (Ansari and Fatma, 2016;
70 Monshupanee and Incharoensakdi, 2014; Rueda et al., 2022a, 2020b; Sharma and
71 Mallick, 2005b). These studies examined the effect of different operation factors on
72 PHB production, such as culture conditions (*e.g.* photoautotrophic, mixotrophic or
73 photoheterotrophic). Results showed that under photoheterotrophic regime, PHB
74 production is enhanced reaching values up to 30 %dcw (Rueda et al., 2022a), making
75 the process a possible candidate for industrial application.

76 A mixed culture enriched with cyanobacteria would in effect combine the
77 aforementioned advantages of working with microbiomes and cyanobacteria, potentially
78 overcoming the production rates obtained by cyanobacteria monocultures up to now.
79 Nevertheless, to the authors' knowledge, photosynthetic microbiomes enriched with
80 cyanobacteria have only been tested for PHB production in (Altamira-Algarra et al.,
81 2022; Arias et al., 2018; Rueda et al., 2020c), obtaining a PHB production up to 14
82 %dcw PHB (Altamira-Algarra et al., 2022). In (Altamira-Algarra et al., 2022) the effect
83 of the number of days under light and the presence of inorganic and organic carbon on
84 PHB production by a photosynthetic microbiome was evaluated. Outcomes revealed
85 that the addition of an organic carbon source (acetate) greatly triggered biopolymer
86 synthesis and reactors could be under dark during PHB production. the presence of
87 inorganic carbon (as bicarbonate) had no notable impact on biopolymer synthesis.
88 These findings were used to establish the operating procedure in a next step using
89 reactors with higher volumes, as well as, to evaluate the feasibility of increasing PHB
90 production by enhancing the presence of organisms producing the biopolymer.

91 In addition, one research gap that needs to be addressed is how to maintain productive
92 cyanobacterial cultures for the long-term generation of bioproduct. Unfortunately, most
93 research undertaken to date has been limited to small-scale experiments with a short
94 time frame, typically lasting only a few weeks. There have been no attempts to maintain
95 cultures in the long term (on the order of several months) for continuous bioproduct

96 generation, which is of important value for industrialization of bioproduct synthesis.
97 Thus, in this work, a photosynthetic microbiome was cultivated in a photobioreactor
98 with a sequential operation for a total of 179 days. The study evaluated a novel
99 methodology based on the FF strategy to enhance with PHB-producers a microbiome
100 rich in cyanobacteria.

101

102 **2. Material and methods**

103 2.1. Inoculum and experimental set-up

104 Microbiome named CC, isolated in (Altamira-Algarra et al., 2022) was used as the
105 inoculum in 3 L glass cylindrical photobioreactors (PBRs) of 2.5 L working volume
106 (Fig. A.1). This microbiome sample was collected from the Canal dels Canyars outlet
107 (Gavà, Spain, 41°15'55.9"N 2°00'39.7"E), very near to the sea, and it was rich in the
108 unicellular cyanobacteria *Synechococcus* sp. and the filamentous cyanobacteria
109 *Leptolyngbya* sp. (Fig. A2). Illumination in reactors was kept at 30 klx (approx. 420
110 $\mu\text{mol}\cdot\text{m}^{-2}\cdot\text{s}^{-1}$) by 200W LED floodlight, placed at 15 cm from the reactors surface in
111 15:9 h light:dark cycles. pH was measured online with a pH probe (HI1001, HANNA
112 instruments, Italy) placed inside the reactors and was controlled at around 7.5 (during
113 growth phase) by a pH controller (HI 8711, HANNA instruments, Italy) activating an
114 electrovalve which injected CO₂ inside the reactors when pH reached 8.5. The pH data
115 was saved in a 5 min interval in a computer with the software PC400 (Campbell
116 Scientific). In the PHB-accumulation phases the pH was measured but not controlled in
117 order to avoid IC presence. Reactors were continuously agitated by a magnetic stirrer
118 ensuring a complete mixing and culture temperature was kept at 30 °C or 35 °C
119 according to the test conditions.

120 2.2. Experimental strategy

121 A novel procedure based on the FF strategy used in PHB production by heterotrophic
122 cultures was applied to the microbiome CC. PBRs were operated for 179 days during
123 which growth/starvation phases were constantly conducted with the aim to enrich the
124 microbiome with PHB-producers' microorganisms.

125 The PBRs were operated in semi-continuous regime. In a first conditioning period,
126 cultures were grown by adding bicarbonate (as inorganic carbon, IC) to the medium,

127 and when nitrogen (N) was depleted, a first PHB-accumulation phase started. Secondly,
128 three cycles consisting of (i) growth and (ii) starvation phases were done to determine
129 the optimal operating conditions to favour cyanobacteria growth together with PHB
130 production. For that, the effect of three ecological stresses (i) N concentration; (ii)
131 temperature and (iii) light were also evaluated. Each parameter was tested individually
132 in one cycle. Finally, after establishing the best results for each parameter, 9 iterated
133 repetitions of (i) growth and (ii) starvation phases were conducted to enrich the biome
134 in PHB-producers. Note that only in the beginning of the first growth phase (in
135 conditioning period) bicarbonate was supplemented to the medium.

136 Experiment was conducted as follows (Fig. 1, and for its description see the text below):

137 i. Conditioning period.

138 Two PBRs were used here as duplicates:

- 139 • Growth phase: the PBRs were inoculated with 100 mg biomass (as volatile
140 suspended solids, VSS)·L⁻¹. BG-11 with modified concentrations of inorganic
141 carbon (IC), N and P (100 mgIC·L⁻¹ (expressed as C), 50 mgN·L⁻¹ and 1 mgP·L⁻¹)
142 was used as media for culture growth.
- 143 • Starvation phase: this step began when N was depleted. 600 mg acetate (Ac)·L⁻¹
144 was added at this point and PBRs were enclosed with PVC tubes to keep the
145 reactors under dark conditions. This first starvation phase was kept for 14 days.

146
147 ii. Cycles period.

148 Three cycles of (i) growth and (ii) starvation phases were conducted with 4 PBRs
149 (duplicates for each parameter tested).

150
151 Cycle 1: Evaluation of N concentration during the growth phase.

- 152 • Growth phase: First, biomass from the two PBR of the prior phase was mixed
153 and divided based in volume in four PBRs. Initial biomass concentration was set
154 at approximately 400 mgVSS·L⁻¹ in the PBRs. Biomass was cultured with new
155 BG-11 medium with modified concentrations of N and P, and without IC. N
156 concentration was set at 25 mgN·L⁻¹ for two PBRs, while the other two were
157 inoculated with medium to have 50 mgN·L⁻¹. P concentration was set at 0.1
158 mg·L⁻¹ due to the sudden growth of green algae during the conditioning revealed

159 by microscope observations. P was daily added to the medium to maintain 0.1
160 $\text{mg}\cdot\text{L}^{-1}$ in the PBRs (Table 1). The P was maintained during the whole growth
161 phase by daily dosing a P solution of KH_2PO_4 to the PBRs.

162 • Starvation phase: The same operation mode was applied as in the starvation
163 phase from the conditioning period. This phase and the coming starvation phases
164 lasted 7 days.

165

166 Cycle 2: Evaluation of temperature during the starvation phase.

167 • Growth phase: A certain volume of the PBRs usually ranging from 800 mL to
168 1,200 mL was discarded to purge the culture broth. The removed volume was
169 calculated to set $400 \text{ mgVSS}\cdot\text{L}^{-1}$ as initial biomass concentration in the PBRs
170 (similar to cycle 1). Discarded volume was replaced with new BG-11 medium
171 with modified concentrations of N and P, and without IC (as bicarbonate). N
172 concentration was set at $25 \text{ mgN}\cdot\text{L}^{-1}$ (best result from the prior cycle) and P, at
173 $0.1 \text{ mg}\cdot\text{L}^{-1}$.

174 • Starvation phase: Two reactors were set at 30°C and the other two, at 35°C . The
175 other parameters were as in the conditioning phase.

176

177 Cycle 3: Evaluation of light during the starvation phase

178 • Growth phase: Equal operation mode as in cycle 2.

179 • Starvation phase: Two reactors were enclosed with PVC tubes for dark
180 conditions while the other two were maintained in light:dark cycles as described
181 before. Temperature was maintained at 35°C (best result from prior cycle).

182

183 iii. Iterated period.

184 A total of nine growth and starvation phases were conducted with the optimal values
185 for the evaluated factors (N, temperature and light) obtained from the cycles period
186 (Table). Biomass from PBR 1 & 2 from the prior phase was mixed and divided in
187 two PBRs, while biomass from PBR 3 & 4 was discarded, thus 2 PBR were used in
188 these cycles. A total of 9 iterated cycles of (i) growth and (ii) starvation phase were
189 conducted. At the beginning of each growth phase, volume ranging from 800 mL to
190 1,200 mL was discarded to purge the culture broth and set $400 \text{ mgVSS}\cdot\text{L}^{-1}$ as initial

191 biomass concentration in the PBRs (as in the previous cycles). Discarded volume
192 was replaced with new BG-11 medium with modified concentrations of N and P,
193 and without IC. Two PBRs were used as replica.

194 2.3. Analytical methods

195 At selected times, a 50 mL sample was taken from each PBR for analysis. Biomass
196 concentration was determined by analysis of total suspended solids (TSS) and VSS as
197 described in (American Public Health Association, 2012). Turbidity was measured with
198 turbidimeter (HI93703, HANNA Instruments). For a quick estimation of biomass
199 content, VSS and turbidity were correlated by calibration curve (Fig. A.3):

200 To determine dissolved species, samples taken out from the reactors were previously
201 filtered through a 0.7 μm pore glass microfiber filter. Nutrients (N and P) were
202 measured as nitrate (N-NO_3^-) and phosphate (P-PO_4^{3-}) following Standard Methods
203 (American Public Health Association, 2012). Note that in BG-11 the only source of N is
204 nitrate. The filtered sample was passed through a 0.45 μm pore size filter a second time
205 to determine Ac by ion chromatography (CS-1000, Dionex Corporation, USA).

206 Biomass composition was monitored by bright light and fluorescence microscope
207 observations (Eclipse E200, Nikon, Japan). Cyanobacteria and green algae were
208 identified and classified following morphological descriptions (Komárek et al., 2020,
209 2011). Cell counting was done in a Neubauer chamber at the end of each starvation
210 phase. Individual cells were counted until reach >400 cells to have a standard error
211 lower than 5 % (Margalef, 1984).

212 2.4. PHB extraction and quantification

213 PHB analysis was adapted from methodology described in (Lanham et al., 2013).
214 Briefly, 50 mL of mixed liquor were collected and centrifuged (4,200 rpm, 7.5 min),
215 frozen at -80 °C overnight in an ultra-freezer (Arctiko, Denmark) and finally freeze-
216 dried for 24 h in a freeze dryer (-110 °C, 0.05 hPa) (Scanvac, Denmark). 3-3.5 mg of
217 freeze-dried biomass were mixed with 1 mL CH_3OH with H_2SO_4 (20% v/v) and 1 mL
218 CHCl_3 containing 0.05 % w/w benzoic acid. Samples were heated for 5 h at 100 °C in a
219 dry-heat thermo-block (Selecta, Spain). Then, they were placed in a cold-water bath for
220 30 min to ensure they were cooled. After that, 1 mL of deionized water was added to the
221 tubes and they were vortexed for 1 min. CHCl_3 phase, containing PHB dissolved, was
222 recovered with a glass pipette and introduced in a chromatography vial containing

223 molecular sieves. Samples were analysed by gas chromatography (GC) (7820A, Agilent
224 Technologies, USA) using a DB-WAX 125-7062 column (Agilent, USA). Helium was
225 used as the gas carrier (4.5 mL·min⁻¹). Injector had a split ratio of 5:1 and a temperature
226 of 230 °C. FID had a temperature of 300 °C. A standard curve of the co-polymer PHB-
227 HV was used to quantify the PHB content.

228 2.5. Calculations

229 Total biovolumes (BV) in mm³·L⁻¹ of each species (cyanobacteria (*Synechococcus* sp.)
230 and the green microalgae) were calculated using the formula:

$$231 \text{ BV} = \frac{n \cdot v}{10^6} \text{ (Eq. 1)}$$

232 where n is the number of cells counted in a sample (cells·L⁻¹) and v is the volume of
233 each cell (μm³). 10⁶ is the unit conversion from μm³·mL to mm³·L⁻¹. Cell volume was
234 calculated by volumetric equations of geometric shape closest to cell shape. Biovolume
235 of *Synechococcus* sp. was calculated by the volume equation of a cylinder and
236 biovolume of green algae was obtained by the volume equation of an ellipsoid. Cell
237 dimensions (length and width) were obtained from images of microscope observations
238 (software NIS- Element viewer®) (Table A1).

239 Kinetic coefficients were calculated as follows:

240 Specific growth rate (d⁻¹) was calculated using the general formula

$$241 \mu_X = \frac{\ln(x)_{t_i} - \ln(x)_{t_0}}{t_i - t_0} \text{ (Eq. 2)}$$

242 where ln(X)_{ti} and ln(X)_{t0} are the natural logarithms of the biomass concentration
243 (mgVSS·L⁻¹) at experimental day (t_i) and at the beginning of the phase (t₀), respectively.
244 The terms t_i and at t₀ are the time span (in days) at which μ_X was calculated (when
245 biomass concentration reached stationary phase).

246 Biomass volumetric production rate (mg·L⁻¹·d⁻¹) was calculated as:

$$247 r_X = \frac{X_{t_i} - X_{t_0}}{t_i - t_0} \text{ (Eq. 3)}$$

248 where X_{ti} (mg·L⁻¹) and X_{t0} (mg·L⁻¹) are the biomass concentration (in mgVSS·L⁻¹) at
249 time t_i (experimental day, when cell growth reached stationary phase) and at the

250 beginning of the growth phase (t_0). i is the total number of days that the growth phase
251 lasted.

252 The nutrients (nitrogen) to biomass yield was calculated by (only during the growth
253 phase):

$$254 \quad Y_{X/N} = \frac{X_{t_n} - X_{t_0}}{N_{t_n} - N_{t_0}} \quad (\text{Eq. 4})$$

255 where X_{t_n} ($\text{mg}\cdot\text{L}^{-1}$) and X_{t_0} ($\text{mg}\cdot\text{L}^{-1}$) are the biomass concentration (in $\text{mgVSS}\cdot\text{L}^{-1}$) at the
256 end (t_n) and at the beginning of the phase (t_0). N_{t_n} ($\text{mg}\cdot\text{L}^{-1}$) and N_{t_0} ($\text{mg}\cdot\text{L}^{-1}$) are the
257 nitrogen concentration (N-NO_3^-) at the end and at the beginning of each growth phase,
258 respectively.

259 The specific consumption rate of nitrogen ($\text{mgN}\cdot\text{mgVSS}^{-1}\cdot\text{d}^{-1}$) was calculated as:

$$260 \quad q_{X/N-\text{NO}_3} = \frac{\mu_X}{Y_{X/N}} \quad (\text{Eq. 5})$$

261 PHB volumetric production rate (\square_{PHB} ($\text{mgPHB}\cdot\text{L}^{-1}\cdot\text{d}^{-1}$)) was obtained by:

$$262 \quad P_{\text{PHB}} = \frac{(\%_{\text{dcwPHB}})_{t_i} \cdot X_{t_i} - (\%_{\text{dcwPHB}})_{t_0} \cdot X_{t_0}}{t_i - t_0} \quad (\text{Eq. 6})$$

263 where $\%_{\text{dcwPHB}})_{t_n}$ and $\%_{\text{dcwPHB}})_{t_i}$ are the percentage of PHB respect biomass
264 quantified at time i (experimental day) and at the beginning of the accumulation phase
265 (t_0). X_{t_i} and X_{t_0} are the biomass concentration (in $\text{mgVSS}\cdot\text{L}^{-1}$) at time i (experimental
266 day) and at the beginning of the accumulation phase (t_0), respectively.

267 The PHB yield on acetate (Ac) ($Y_{\text{PHB}/\text{Ac}}$) was calculated on a COD-basis by:

$$268 \quad Y_{\text{PHB}/\text{Ac}} = \frac{\text{PHB}_{t_i} - \text{PHB}_{t_0}}{\text{Ac}_{t_i}} \quad (\text{Eq. 7})$$

269 The amount of PHB produced (given as chemical oxygen demand (COD): 1.67
270 $\text{gCOD}\cdot\text{gPHB}^{-1}$) was obtained by multiplying the $\%_{\text{dcwPHB}}$ produced per biomass
271 concentration (in $\text{mgVSS}\cdot\text{L}^{-1}$) at time i (experimental day) and at the beginning (t_0) of
272 the accumulation phase. Ac_{t_i} ($\text{mg}\cdot\text{L}^{-1}$) is the acetate concentration (given 1.07
273 $\text{gCOD}\cdot\text{gAc}^{-1}$) at the experimental day (t_i) of the starvation phase. Ac_{t_i} was calculated by
274 subtracting the amount added ($600 \text{ mgAc}\cdot\text{L}^{-1}$) from the amount of acetate left in the
275 medium.

276

277

278 3. Results and discussion

279 3.1. Conditioning period

280 A first growth phase with $100 \text{ mgIC}\cdot\text{L}^{-1}$ (added as bicarbonate), $50 \text{ mgN}\cdot\text{L}^{-1}$ and 1
281 $\text{mgP}\cdot\text{L}^{-1}$ to reach a clearly detectable growth and biomass concentration was conducted.
282 The average specific growth rate was 0.31 d^{-1} (Table 2) and after 7 days the microbiome
283 grew up to $1,120 \text{ mgVSS}\cdot\text{L}^{-1}$ (Fig. 2A and Table 2). Nitrogen was assimilated during
284 this growth phase at a specific consumption rate of $15 \text{ mgN}\cdot\text{gVSS}^{-1}\cdot\text{d}^{-1}$ (Table 2). These
285 values were in accordance with previous work with monocultures of cyanobacteria
286 under similar culture conditions (Rueda et al., 2022a, 2022b).

287 After seven days of reactor operation, N was depleted (Fig. 2A) and $600 \text{ mgAc}\cdot\text{L}^{-1}$ were
288 added to the medium. This first starvation phase was maintained 14 days in order to
289 follow PHB synthesis (Fig. 2B). Biomass concentration remained constant during this
290 period (Fig. 2A). Regarding to biopolymer synthesis, it increased until day 7 in
291 starvation, when 1.5 %dcw PHB was produced in both PBRs. However, from that day
292 on, biopolymer synthesis decreased, and after 14 days in starvation, there was almost no
293 PHB present; probably due to depletion of Ac and the consumption of the produced
294 PHB. Consequence of this result, subsequent starvation phases lasted one week to avoid
295 PHB consumption under dark, which would not favour growth of photosynthetic PHB-
296 producers. Note that in this period the PHB synthesis was comparatively low.

297 The two PBRs were inoculated with a microbiome rich in the unicellular cyanobacteria
298 *Synechococcus* sp. and the filamentous cyanobacteria *Leptolyngbya* sp. Unfortunately, a
299 sudden growth of green algae was observed during this conditioning period (Fig. A.2).
300 In fact, BV calculation disclosed that 80 % of the culture was composed by these
301 microalgae. Consequently, to avoid green microalgae and favour cyanobacteria growth,
302 P concentration at the beginning of each growth phase was fixed at $0.1 \text{ mg}\cdot\text{L}^{-1}$. Note
303 that the biomass used as inoculum for the PBRs had been kept in modified BG-11
304 medium with a P concentration of $0.5 \text{ mg}\cdot\text{L}^{-1}$ (Altamira-Algarra et al., 2022). The P
305 concentration set at the beginning of the conditioning period was $1 \text{ mgP}\cdot\text{L}^{-1}$ to sustain
306 cell growth; however, we assumed that this value was too high and P stopped being
307 growth-limiting for green algae.

308 3.2. Growth and PHB production under ecological stress

309 The conditioning period was done to obtain sufficient biomass concentration in the
310 PBRs and initiate a first PHB accumulation step, which we assumed it would serve as
311 the internal biopolymer for cell growth on the coming growth phase. After fourteen
312 days in starvation (accumulation phase of the conditioning phase), biomass was equally
313 divided into four PBRs and three cycles of (i) growth and (ii) starvation were
314 conducted. In these cycles, the effect of N concentration at the beginning of the growth
315 phase (cycle 1), temperature (cycle 2) and light (cycle 3) at the starvation phase was
316 assessed.

317

318 To do so, no IC (as bicarbonate) was added at the growth phase to create a selection
319 pressure favourable for microorganisms with the capacity to store PHB, because they
320 would use the accumulated biopolymer during the starvation phase as an internal carbon
321 source (Reis et al., 2011). However, CO₂ was injected in the PBRs to control pH due to
322 photosynthetic activity. Note that this CO₂ presence, even small, is beneficial for
323 biopolymer degradation, as cells need to resume photosynthetic activity in order to use
324 the stored PHB (Klotz et al., 2016).

325

326 To support the growth on internal PHB, nutrients are required; thus, two N
327 concentrations were evaluated (cycle 1). In two PBRs (PBR 1 and PBR 2) N
328 concentration was lowered to 25 mgN·L⁻¹ and in the other two PBRs (PBR 3 and PBR
329 4), N concentration was 50 mgN·L⁻¹, the same as in the first growth phase (conditioning
330 period). Biomass increased from 400 mgVSS·L⁻¹ to 670 ± 100 mgVSS·L⁻¹ in PBR 1 & 2
331 in seven days, and up to 1,300 ± 140 mgVSS·L⁻¹ in PBR 3 & 4 in nine days (Fig. 3A
332 and Table 2). The increase in biomass and the calculated kinetic parameters (Table 2
333 and Table 3) were higher in the latter PBRs because initial N concentration was also
334 major (50 mgN·L⁻¹). However, PHB production and productivity were lower (Table 3).
335 In addition, by lowering N concentration at the beginning of the growth phase, this
336 phase could be shortened to seven days; thus, reducing the days of the whole process, as
337 700 ± 100 mgVSS·L⁻¹ was considered to be enough biomass concentration to start the
338 accumulation step for next experiments. Therefore, N concentration was set at 25 mg·L⁻¹
339 at the beginning of each growth phase, and it lasted 7 days.

340 Although the initial N concentration in the growth phase of the conditioning period was
341 equal as that settled for PBR 3 & 4 in cycle 1 (50 mg·L⁻¹), the biomass grew faster

342 during the growth phase of the conditioning period ($\mu = 0.31 \text{ d}^{-1}$) than in the same phase
343 in cycle 1 in PBR 3 & 4 ($\mu = 0.21 \text{ d}^{-1}$). This difference in biomass growth could be
344 attributed to the higher P concentration in the conditioning period ($1 \text{ mg}\cdot\text{L}^{-1}$) and the
345 sudden increase in green algae, which tend to grow faster than cyanobacteria (Visser et
346 al., 2016). This would suggest that the biomass ($1,120 \text{ mgVSS}\cdot\text{L}^{-1}$) in the conditioning
347 period was mainly composed by green algae and in lower concentration by
348 cyanobacteria. Moreover, it is worth noting that throughout the cycles, growth rate (μ)
349 decreases (Table 3), while there was an increase in cyanobacteria through this period
350 (Fig. 4A). Also, this reduction in cell growth could be attributed to the absence of
351 external IC as bicarbonate during these growth phases, which is the primary source of
352 inorganic carbon for autotrophic organisms in aquatic environments (Salbitani et al.,
353 2020). While $100 \text{ mgIC}\cdot\text{L}^{-1}$ were added in the growth phase of the conditioning period,
354 no IC was added during the cycles period; thus, cell relied on alternative sources of
355 carbon (PHB) to support their metabolic needs. This could slow down the overall rate of
356 growth (Table 3), as these stored materials may not be as readily available or efficient as
357 bicarbonate as a source of carbon.

358

359 The effects of temperature and light during the starvation phase were also asset in cycle
360 2 and cycle 3, respectively. Temperature was controlled at 35°C in PBR1 & 2 and at
361 30°C in PBR 3 & 4. As observed in the previous growth phase (from cycle 1), N was
362 consumed in 7 days and biomass reached values of $780 \pm 100 \text{ mgVSS}\cdot\text{L}^{-1}$ in all the
363 PBRs in cycle 2 and $800 \pm 40 \text{ mgVSS}\cdot\text{L}^{-1}$ in cycle 3 (Fig. 3B). Nutrients intake also
364 suggests that the stored PHB was being consumed. The PHB concentration decreased
365 from the last day of starvation phase in cycle 1 to the beginning of the starvation phase
366 in cycle 2; and from the last day of starvation phase in cycle 2 to the beginning of the
367 starvation phase in cycle 3 were observed (Fig. 4C), meaning that the biopolymer was
368 being consumed as a carbon source for cell growth. This observation was also supported
369 by nitrogen intake in each growth phase (Fig. 3A and 3B).

370 Outcomes revealed that to promote PHB production, the best temperature was 35°C in
371 order to favour cyanobacterial while decreasing green algae growth, as PHB synthesis
372 was higher in PBR 1 & 2 than in PBR 3 & 4 (Fig. 4 and Table 3). Moreover, the
373 concentration of green algae, which had already decreased since P concentration was set
374 at $0.1 \text{ mg}\cdot\text{L}^{-1}$ from cycle 1 onwards, continued to decrease until approximately 30% at

375 the end of cycle 3 in PBR 1 & 2 (Fig.4A, 4B and A.4), demonstrating the predominance
376 of cyanobacteria over green algae by the increase in temperature. Cyanobacteria
377 concentration domination over green-algae by warming has also been described in
378 (Lürling et al., 2018, 2013).

379 Results from cycle 3 showed that reactors should also be enclosed, meaning that no
380 light was needed for PHB synthesis, which was in accordance with the result obtained
381 in the Design of Experiment conducted in (Altamira-Algarra et al., 2022) with the used
382 microbiome. The assumption that light is not required for PHB production has been
383 proved before due to anoxic environment caused by dark cultivation conditions since
384 photosynthetic oxygen is not produced in the dark (Koch et al., 2020; Sharma and
385 Mallick, 2005a). This could be partially related to the increased pool of NADPH under
386 dark (Pelroy et al., 1976), which is necessary for PHB biosynthesis (García et al., 2018;
387 Hauf et al., 2013). Here, a notorious difference in PHB was observed between PBRs.
388 Production in the non-enclosed PBRs was $0.75 \%dcw \pm 0.21$, the lowest observed in all
389 the performed cycles (Fig. 4C and Table 3). In addition, from the $600 \text{ mgAc}\cdot\text{L}^{-1}$ added
390 in the four PBRs, biomass from PBR 1& 2 consumed almost all of it ($500 \text{ mgAc}\cdot\text{L}^{-1} \pm$
391 35.7), while that from PBR 3 & 4 only consumed $124 \text{ mgAc}\cdot\text{L}^{-1} \pm 8.63$.

392 3.3. Growth and PHB production under optimal operating conditions

393 Outcomes from the three cycles performed to study the effect of three ecological
394 stresses (N concentration, temperature and light) established the operation mode for the
395 next period, which was performing nine iterated cycles of biomass growth followed by
396 PHB accumulation phase. These repetitions consisted of seven days of growing and
397 seven days of PHB synthesis (Fig. 1).

398 Here two PBRs were used with the biomass from the prior PBR 1 & 2, as it was the
399 culture with higher PHB production in the previous cycle (Table 3). Biomass increased
400 from 400 to approximately $745 \text{ mgVSS}\cdot\text{L}^{-1}$ in both PBRs with the addition of 25
401 $\text{mgN}\cdot\text{L}^{-1}$ and $0.1 \text{ mgP}\cdot\text{L}^{-1}$ after seven days in all the repetitions (Table 4). A PHB
402 decrease was always observed between the end of one accumulation phase (repetition n)
403 and the beginning of the next accumulation phase (repetition $n+1$) (Fig. 5C); suggesting
404 that during each growth phase, biomass used the stored PHB as carbon source, together
405 with the external N and P to support cell growth, as already observed in the prior cycles
406 and also by other authors (Johnson et al., 2009; Serafim et al., 2004). This trend is more

407 clearly observed when the PHB concentrations reached at the end of the accumulation
408 phase are somewhat low. When PHB is higher, the biopolymer concentration at the end
409 of the growth phase is also higher, suggesting that not all PHB has been consumed.

410 In the first repetition, both PBRs had similar behaviour on PHB production (Fig. 5C).
411 However, production by PBR 1 increased to 13.4 %dcw in the second repetition and
412 remained in similar values at every new accumulation phase until the fifth iterated cycle
413 (Fig. 5C). Curiously, PHB production in PBR 1 decreased to < 5 %dcw from the sixth
414 accumulation onwards (Fig. 5C and Table 5). In PBR 2, PHB production did not
415 underwent such a sudden rise; instead the microbiome did not produce more than 10
416 %dcw PHB until the repetition number eight, when PHB production was 13.2 %dcw
417 (Fig. 5C). By the end of the last accumulation, PHB production was 22 %dcw (Fig. 5C
418 and Table 5). Similarly, (Rueda et al., 2022a) achieved a biopolymer production rate of
419 26 %dcw with a monoculture of *Synechococcus* sp. with the addition of Ac after 15
420 days of accumulation.

421 Regarding to Ac consumption, in PBR 1 half of the Ac remained in the media after
422 seven days in the first repetition (Table A.2). Interestingly, at each new accumulation,
423 the acetate consumed was greater, which should be attributed to an also higher
424 biopolymer production (Table A.2). However, as mentioned, an increase in PHB did not
425 occur (Fig. 5C), suggesting that Ac was not exclusively used for PHB synthesis. This
426 consideration can also be seen by the $Y_{\text{PHB}/\text{Ac}}$, which remained constant until repetition
427 8 and 9, when it suddenly dropped (Table 5). Contrary, in PBR 2, where cyanobacteria
428 were more prevalent than green microalgae (Fig. 5), the concentration of Ac by the end
429 of each repetition remained around $100 \text{ mg}\cdot\text{L}^{-1}$. The highest $Y_{\text{PHB}/\text{Ac}}$ was obtained in
430 repetition 9 (Table 5). However, the theoretical maximum $Y_{\text{PHB}/\text{Ac}}$ that could be reached
431 by consuming $600 \text{ mgAc}\cdot\text{L}^{-1}$ is 0.60, which represents 52 %dcw PHB assuming biomass
432 concentration of $745 \text{ mgVSS}\cdot\text{L}^{-1}$ (the average VSS produced during the iterated cycles
433 considering both PBRs). Here lower yields were obtained (Table 5), which suggests the
434 possibility of optimizing Ac uptake by changing substrate addition, in order to increase
435 PHB production and avoid an external carbon source in the coming growth phase. In
436 this sense, one possibility could be continuous substrate feeding or pulse-wise addition.
437 Notably, despite these differences in Ac uptake, pH during accumulation phase
438 remained quite constant in values around 8 in both PBRs after a few days (Fig. A.5).

439 Interestingly, cyanobacteria proportion in PBR 1 remained quite constant until
440 repetition 6, where it suffered a decrease from 73 % at the end of repetition 5 to 46 % at
441 the end of the sixth repetition. By the end of repetition 9, green algae were clearly
442 dominant in this microbiome (Fig. 5A). The reduction in $Y_{\text{PHB}/\text{Ac}}$, due to lower PHB
443 production and Ac uptake, seems to be linked with this decrease in cyanobacteria
444 dominance and the increase in green algae in PBR 1 (Fig. 5). Furthermore, the
445 microbiome composition of PBR 2 remained similar from repetition 1 to 7 (63 %
446 cyanobacteria and 37 % green algae) (Fig. 5B). By the end of repetition 7, the % of
447 cyanobacteria increased to 83 % and was still high for repetitions 8 and 9 (Fig. 5B),
448 which agreed with the observed increment with biopolymer production and $Y_{\text{PHB}/\text{Ac}}$
449 (Fig. 5C and Table 5).

450 The presented data clearly demonstrates that the microbiome's composition, which
451 includes cyanobacteria and green algae, led to significant variations in the PHB results.
452 This is likely due to the fact that green algae are non-PHB-producers with a greater BV
453 (and weight) than PHB-producers (cyanobacteria). (Fradinho et al., 2013b) tested a
454 photosynthetic mixed culture (bacteria and algae) which produced 30 %dcw PHB due to
455 the lower number of algae present in the culture compared to a 20 %dcw PHB
456 production in a previous test with the same culture (Fradinho et al., 2013a). (Arias et al.,
457 2017), who also worked with a mixed culture composed by green algae and
458 cyanobacteria, observed that PHB was not accumulated by the lack of cyanobacteria in
459 their cultures. The variations in PHB production (Fig. 5A) suggest that the microbiome
460 may have produced more PHB than what was detected, which highlights the high
461 capacity of the microbiome to produce this biopolymer.

462 Although the PBRs were replicas and subjected to the same operation procedures, they
463 resulted in different outcomes. These differences arise from small deviations in
464 macroscopic variables that are often imperceptible to the researchers. Such variations
465 can lead to changes at the microscopic level that ultimately affect bioproduct results.
466 For example, in our case, it is possible that slight variations in pH regulation (Fig. A5)
467 or differences in lighting, based on the PBRs placement, could condition the evolution
468 of the microbial populations. Therefore, meticulous control is necessary to ensure the
469 reliability of the bioprocessing, regardless of the richness of the microbiome.

470 **4. Conclusions**

471 The experimental data demonstrated a substantial increase in PHB production from 2
472 %dcw PHB in the first phase to 22 %dcw PHB after a total of 179 days of reactor
473 operation. These findings suggest the successful development of biopolymer-producing
474 biomass. However, the presence of green algae led to a decline in PHB production,
475 posing a challenge to maintaining consistent production rates. Although operational
476 parameters such as P concentration or temperature could potentially control the survival
477 of green algae, their abundance sometimes exceeds the controllable limits. This
478 highlights the importance of implementing effective strategies to monitor and manage
479 the growth of competing microorganisms in the reactor.

480 The results indicate that this strategy could offer a new methodology to enrich a
481 photosynthetic microbiome in PHB-producers. This discovery could pave the way for
482 more efficient PHB production strategies in the future, while also minimizing the
483 growth of unwanted microorganisms in the reactor.

484 **CRedit authorship contribution statement**

485 **Beatriz Altamira-Algarra:** Conceptualization, Validation, Formal analysis,
486 Methodology, Investigation, Writing – original draft. **Artai Lage:** Methodology. **Joan**
487 **Garcia:** Conceptualization, Resources, Writing – review & editing, Supervision, Project
488 administration, Funding acquisition. **Eva Gonzalez-Flo:** Conceptualization,
489 Supervision, Writing – review & editing.

490 **Declaration of Competing Interest**

491 The authors declare that they have no known competing financial interests or personal
492 relationships that could have appeared to influence the work reported in this paper.

493 **Acknowledgements**

494 This research has received funding from the European Union’s Horizon 2020 research
495 and innovation programme under the grant agreement No 101000733 (project
496 PROMICON). B. Altamira-Algarra thanks the Agency for Management of University
497 and Research (AGAUR) for her grant [FIAGAUR_2021]. E. Gonzalez-Flo would like
498 to thank the European Union-Next Generation EU, Ministry of Universities and
499 Recovery, Transformation and Resilience Plan for her research grant [2021UPF-MS-
500 12].

501 **References**

- 502 Altamira-Algarra, B., Rueda, E., Lage, A., San Leon, D., Martinez-Blanch, J.F.,
503 Nogales, J., García, J., Gonzalez-Flo, E., 2022. New strategy for bioplastic and
504 exopolysaccharides production: Enrichment of field microbiomes with
505 cyanobacteria. *New Biotechnol.* Submitted.
- 506 American Public Health Association, 2012. *Standard Methods for the Examination of*
507 *Water and Wastewater*, 22nd ed.
- 508 Ansari, S., Fatma, T., 2016. Cyanobacterial Polyhydroxybutyrate (PHB): Screening,
509 Optimization and Characterization. <https://doi.org/10.1371/journal.pone.0158168>
- 510 Arias, D.M., Fradinho, J.C., Uggetti, E., García, J., Oehmen, A., Reis, M.A.M., 2018.
511 Polymer accumulation in mixed cyanobacterial cultures selected under the feast
512 and famine strategy. *Algal Res.* 33, 99–108.
513 <https://doi.org/10.1016/j.algal.2018.04.027>
- 514 Arias, D.M., Uggetti, E., García-Galán, M.J., García, J., 2017. Cultivation and selection
515 of cyanobacteria in a closed photobioreactor used for secondary effluent and
516 digestate treatment. *Sci. Total Environ.* 587–588, 157–167.
517 <https://doi.org/10.1016/j.scitotenv.2017.02.097>
- 518 Crognale, S., Lorini, L., Valentino, F., Villano, M., Cristina, M.G., Tonanzi, B.,
519 Majone, M., Rossetti, S., 2022. Effect of the organic loading rate on the PHA-
520 storing microbiome in sequencing batch reactors operated with uncoupled carbon
521 and nitrogen feeding. *Sci. Total Environ.* 825.
522 <https://doi.org/10.1016/J.SCITOTENV.2022.153995>
- 523 Estévez-Alonso, Á., Altamira-Algarra, B., Arnau-Segarra, C., van Loosdrecht, M.C.M.,
524 Kleerebezem, R., Werker, A., 2022. Process conditions affect properties and
525 outcomes of polyhydroxyalkanoate accumulation in municipal activated sludge.
526 *Bioresour. Technol.* 364. <https://doi.org/10.1016/j.biortech.2022.128035>
- 527 Fradinho, J.C., Domingos, J.M.B., Carvalho, G., Oehmen, A., Reis, M.A.M., 2013a.
528 Polyhydroxyalkanoates production by a mixed photosynthetic consortium of
529 bacteria and algae. *Bioresour. Technol.* 132, 146–153.
530 <https://doi.org/10.1016/J.BIORTECH.2013.01.050>
- 531 Fradinho, J.C., Oehmen, A., Reis, M.A.M., 2013b. Effect of dark/light periods on the
532 polyhydroxyalkanoate production of a photosynthetic mixed culture. *Bioresour.*

- 533 Technol. 148, 474–479. <https://doi.org/10.1016/j.biortech.2013.09.010>
- 534 García, A., Ferrer, P., Albiol, J., Castillo, T., Segura, D., Peña, C., 2018. Metabolic flux
535 analysis and the NAD(P)H/NAD(P)⁺ ratios in chemostat cultures of *Azotobacter*
536 *vinelandii*. *Microb. Cell Fact.* 17, 1–13. <https://doi.org/10.1186/s12934-018-0860-8>
- 537 Hauf, W., Schlebusch, M., Hüge, J., Kopka, J., Hagemann, M., Forchhammer, K., 2013.
538 Metabolic changes in *Synechocystis* PCC6803 upon nitrogen-starvation: Excess
539 NADPH sustains polyhydroxybutyrate accumulation. *Metabolites* 3, 101–118.
540 <https://doi.org/10.3390/metabo3010101>
- 541 Jendrossek, D., Handrick, R., 2002. Microbial degradation of polyhydroxyalkanoates.
542 *Annu. Rev. Microbiol.* 56, 403–432.
543 <https://doi.org/10.1146/annurev.micro.56.012302.160838>
- 544 Johnson, K., Jiang, Y., Kleerebezem, R., Muyzer, G., Van Loosdrecht, M.C.M., 2009.
545 Enrichment of a mixed bacterial culture with a high polyhydroxyalkanoate storage
546 capacity. *Biomacromolecules* 10, 670–676. <https://doi.org/10.1021/BM8013796>
- 547 Klotz, A., Georg, J., Bučinská, L., Watanabe, S., Reimann, V., Januszewski, W.,
548 Sobotka, R., Jendrossek, D., Hess, W.R., Forchhammer, K., 2016. Awakening of a
549 Dormant Cyanobacterium from Nitrogen Chlorosis Reveals a Genetically
550 Determined Program. *Curr. Biol.* 26, 2862–2872.
551 <https://doi.org/10.1016/j.cub.2016.08.054>
- 552 Koch, M., Berendzen, K.W., Forchhammer, K., 2020. On the role and production of
553 polyhydroxybutyrate (PHB) in the cyanobacterium *Synechocystis* sp. pcc 6803.
554 *Life* 10. <https://doi.org/10.3390/life10040047>
- 555 Komárek, J., Johansen, J.R., Šmarda, J., Strunecký, O., 2020. Phylogeny and taxonomy
556 of *synechococcus*-like cyanobacteria. *Fottea* 20, 171–191.
557 <https://doi.org/10.5507/fot.2020.006>
- 558 Komárek, J., Kaštovský, J., Jezberová, J., 2011. Phylogenetic and taxonomic
559 delimitation of the cyanobacterial genus *aphanothece* and description of *anathece*
560 gen. nov. *Eur. J. Phycol.* 46, 315–326.
561 <https://doi.org/10.1080/09670262.2011.606373>
- 562 Lanham, A.B., Ricardo, A.R., Albuquerque, M.G.E., Pardelha, F., Carvalheira, M.,

- 563 Coma, M., Fradinho, J., Carvalho, G., Oehmen, A., Reis, M.A.M., 2013.
564 Determination of the extraction kinetics for the quantification of
565 polyhydroxyalkanoate monomers in mixed microbial systems. *Process Biochem.*
566 48, 1626–1634. <https://doi.org/10.1016/J.PROCBIO.2013.07.023>
- 567 Lürling, M., Eshetu, F., Faassen, E.J., Kosten, S., Huszar, V.L.M., 2013. Comparison of
568 cyanobacterial and green algal growth rates at different temperatures. *Freshw. Biol.*
569 58, 552–559. <https://doi.org/10.1111/j.1365-2427.2012.02866.x>
- 570 Lürling, M., Mello, M.M., van Oosterhout, F., Domis, L. de S., Marinho, M.M., 2018.
571 Response of natural cyanobacteria and algae assemblages to a nutrient pulse and
572 elevated temperature. *Front. Microbiol.* 9, 1–14.
573 <https://doi.org/10.3389/fmicb.2018.01851>
- 574 Manikandan, N.A., Pakshirajan, K., Pugazhenti, G., 2020. Preparation and
575 characterization of environmentally safe and highly biodegradable microbial
576 polyhydroxybutyrate (PHB) based graphene nanocomposites for potential food
577 packaging applications. *Int. J. Biol. Macromol.* 154, 866–877.
578 <https://doi.org/10.1016/j.ijbiomac.2020.03.084>
- 579 Margalef, R., 1984. *Limnologia*. Ediciones Omega, Barcelona.
- 580 Mohamad Fauzi, A.H., Chua, A.S.M., Yoon, L.W., Nittami, T., Yeoh, H.K., 2019.
581 Enrichment of PHA-accumulators for sustainable PHA production from crude
582 glycerol. *Process Saf. Environ. Prot.* 122, 200–208.
583 <https://doi.org/10.1016/j.psep.2018.12.002>
- 584 Mohammadalipour, M., Asadolahi, M., Mohammadalipour, Z., Behzad, T., Karbasi, S.,
585 2023. Plasma surface modification of electrospun polyhydroxybutyrate (PHB)
586 nanofibers to investigate their performance in bone tissue engineering. *Int. J. Biol.*
587 *Macromol.* 230. <https://doi.org/10.1016/j.ijbiomac.2023.123167>
- 588 Monshupanee, T., Incharoensakdi, A., 2014. Enhanced accumulation of glycogen, lipids
589 and polyhydroxybutyrate under optimal nutrients and light intensities in the
590 cyanobacterium *Synechocystis* sp. PCC 6803. *J. Appl. Microbiol.* 116, 830–838.
591 <https://doi.org/10.1111/jam.12409>
- 592 Oliveira, C.S.S., Silva, C.E., Carvalho, G., Reis, M.A., 2017. Strategies for efficiently
593 selecting PHA producing mixed microbial cultures using complex feedstocks:

- 594 Feast and famine regime and uncoupled carbon and nitrogen availabilities. N.
595 Biotechnol. 37, 69–79. <https://doi.org/10.1016/j.nbt.2016.10.008>
- 596 Pelroy, R.A., Levine, G.A., Bassham, J.A., 1976. Kinetics of light dark CO₂ fixation
597 and glucose assimilation by *Aphanocapsa* 6714. J. Bacteriol. 128, 633–643.
598 <https://doi.org/10.1128/jb.128.2.633-643.1976>
- 599 Reis, M., Albuquerque, M., Villano, M., Majone, M., 2011. Mixed Culture Processes
600 for Polyhydroxyalkanoate Production from Agro-Industrial Surplus/Wastes as
601 Feedstocks, Second Edi. ed, Comprehensive Biotechnology, Second Edition.
602 Elsevier B.V. <https://doi.org/10.1016/B978-0-08-088504-9.00464-5>
- 603 Rueda, E., Altamira-Algarra, B., García, J., 2022a. Process optimization of the
604 polyhydroxybutyrate production in the cyanobacteria *Synechocystis* sp. and
605 *Synechococcus* sp. Bioresour. Technol. 356, 127330.
606 <https://doi.org/10.1016/J.BIORTECH.2022.127330>
- 607 Rueda, E., García-Galán, M.J., Díez-Montero, R., Vila, J., Grifoll, M., García, J., 2020a.
608 Polyhydroxybutyrate and glycogen production in photobioreactors inoculated with
609 wastewater borne cyanobacteria monocultures. Bioresour. Technol. 295, 122233.
610 <https://doi.org/10.1016/j.biortech.2019.122233>
- 611 Rueda, E., García-Galán, M.J., Díez-Montero, R., Vila, J., Grifoll, M., García, J.,
612 2020b. Polyhydroxybutyrate and glycogen production in photobioreactors
613 inoculated with wastewater borne cyanobacteria monocultures. Bioresour. Technol.
614 295, 122233. <https://doi.org/10.1016/j.biortech.2019.122233>
- 615 Rueda, E., García-Galán, M.J., Ortiz, A., Uggetti, E., Carretero, J., García, J., Díez-
616 Montero, R., 2020c. Bioremediation of agricultural runoff and biopolymers
617 production from cyanobacteria cultured in demonstrative full-scale
618 photobioreactors. Process Saf. Environ. Prot. 139, 241–250.
619 <https://doi.org/10.1016/j.psep.2020.03.035>
- 620 Rueda, E., Gonzalez-Flo, E., Roca, L., Carretero, J., García, J., 2022b. Accumulation of
621 polyhydroxybutyrate in *Synechocystis* sp. isolated from wastewaters: Effect of
622 salinity, light, and P content in the biomass. J. Environ. Chem. Eng. 10, 107952.
623 <https://doi.org/10.1016/j.jece.2022.107952>
- 624 Sagastume, F.M., Valentino, F., Hjort, M., Zanolli, G., Majone, M., Werker, A., 2017.

- 625 Acclimation process for enhancing polyhydroxyalkanoate accumulation in
626 activated-sludge biomass. *Waste and Biomass Valorization* 10, 1065–1082.
- 627 Salbitani, G., Bolinesi, F., Affuso, M., Carraturo, F., Mangoni, O., Carfagna, S., 2020.
628 Rapid and positive effect of bicarbonate addition on growth and photosynthetic
629 efficiency of the green microalgae *Chlorella Sorokiniana* (Chlorophyta,
630 Trebouxiophyceae). *Appl. Sci.* 10. <https://doi.org/10.3390/app10134515>
- 631 Serafim, L.S., Lemos, P.C., Oliveira, R., Reis, M.A.M., 2004. Optimization of
632 polyhydroxybutyrate production by mixed cultures submitted to aerobic dynamic
633 feeding conditions. *Biotechnol. Bioeng.* 87, 145–160.
634 <https://doi.org/10.1002/bit.20085>
- 635 Sharma, L., Mallick, N., 2005a. Enhancement of poly- β -hydroxybutyrate accumulation
636 in *Nostoc muscorum* under mixotrophy, chemoheterotrophy and limitations of gas-
637 exchange. *Biotechnol. Lett.* 27, 59–62. <https://doi.org/10.1007/s10529-004-6586-1>
- 638 Sharma, L., Mallick, N., 2005b. Accumulation of poly- β -hydroxybutyrate in *Nostoc*
639 *muscorum*: Regulation by pH, light-dark cycles, N and P status and carbon
640 sources. *Bioresour. Technol.* 96, 1304–1310.
641 <https://doi.org/10.1016/J.BIORTECH.2004.10.009>
- 642 Sruamsiri, D., Thayanukul, P., Suwannasilp, B.B., 2020. In situ identification of
643 polyhydroxyalkanoate (PHA)-accumulating microorganisms in mixed microbial
644 cultures under feast/famine conditions. *Sci. Rep.* 10, 1–10.
645 <https://doi.org/10.1038/s41598-020-60727-7>
- 646 Tan, D., Wang, Y., Tong, Y., Chen, G.Q., 2021. Grand Challenges for Industrializing
647 Polyhydroxyalkanoates (PHAs). *Trends Biotechnol.* 39, 953–963.
648 <https://doi.org/10.1016/j.tibtech.2020.11.010>
- 649 Visser, P.M., Ibelings, B.W., Bormans, M., Huisman, J., 2016. Artificial mixing to
650 control cyanobacterial blooms: a review. *Aquat. Ecol.* 50, 423–441.
651 <https://doi.org/10.1007/s10452-015-9537-0>

652

653 **Figure Captions**

654 **Figure 1.** Schematic representation of the PBR semi-continuous operation applied for
655 microbiome optimization for PHB-producing cyanobacteria populations. In green line is
656 showed the assumed increase in PHB-producers biomass; in red, the assumed PHB
657 evolution over time. Colours below the graph represent the concentration of the main
658 nutrients in the experimental phases. The lighter the colour, the lower the concentration
659 of the compound. Brown colour represents the inorganic carbon (IC) and the organic
660 carbon (OC) concentration; blue colour represents the N and yellow is for P. White and
661 grey colour in the figure indicates growth phase and starvation phase, respectively, in all
662 the figures from this paper.

663 **Figure 2.** (A) Concentration changes in biomass (as volatile suspended solids, VSS)
664 and nitrogen (as N- NO₃) in PBR 1 & 2. (B) PHB production in PBR 1 & 2. Error bars
665 indicate the standard deviation of the replicates. Nitrate was not measured during
666 starvation phase. PHB was not measured in growth phase. Values of biomass (as VSS)
667 were obtained following (American Public Health Association, 2012).

668 **Figure 3.** Concentration changes in biomass (as volatile suspended solids, VSS) and
669 nitrogen (as N- NO₃) in PBR 1 & 2 (orange) and PBR 3 & 4 (green) (A) during cycle 1
670 and (B) during cycle 2 and 3. First dashed line in (A) indicates the beginning of
671 starvation phase in PBR 1 & 2; second dashed line stands for PBR 3 & 4. Continuous
672 black line in (B) illustrates end of cycle 2 and beginning of cycle 3. Values of biomass
673 (as VSS) were obtained by turbidity measurements.

674 **Figure 4.** Biovolumes of (A) PBR 1 & 2 and (B) PBR 3 & 4 during the cycle period.
675 (C) PHB evolution in the cycle period. PHB was not measured in growth phase.

676 **Figure 5.** (A) Biovolume of (A) PBR1 and (B) PBR2 during the iterated period. (C)
677 PHB evolution in the iterated period. PHB was not measured in growth phase.

678 **Tables**

679

680

Table 1. Stabilished conditions used in each period of the experiment.

Period	Phase	N (mg·L ⁻¹)	P (mg·L ⁻¹)	Ac (mg·L ⁻¹)	Lightness (h of light:dark)	T (°C)	Number of PBR
Conditioning	Growth	50	1	-	15:09	30	2
	Starvation	-	-	600	0	30	2
Cycle 1	Growth	25 (PBR 1 & 2) 50 (PBR 1 & 2)	0.1	-	15:09	30	4
	Starvation	-	-	600	0	35	4
Cycle 2	Growth	25	0.1	-	15:09	30	4
	Starvation	-	-	600	0	35 (PBR 1 & 2) 30 (PBR 3 & 4)	4
Cycle 3	Growth	25	0.1	-	15:09	30	4
	Starvation	-	-	600	0 (PBR 1 & 2) continuous (PBR 3 & 4)	35	4
Iterated period	Growth	25	0.1	-	15:09	30	2
	Starvation	-	-	600	0	35	2

682 **Table 2.** Average of the kinetic and stoichiometric parameters obtained during growth
 683 and accumulation phase of the conditioning period.

Growth phase	
Parameter	PBR 1 & 2
VSS (mg·L ⁻¹) *	1,120
μ (d ⁻¹) *	0.31
\square_{biomass} (mgVSS·L ⁻¹ ·d ⁻¹)	92.92
q_N (mgN·gVSS ⁻¹ ·d ⁻¹)	15.35
$Y_{X/N}$	20.45
Accumulation phase	
Parameter ^a	PBR 1 & 2
PHB (%dcw)	1.47 ± 0.04
\square_{PHB} (mgPHB·L ⁻¹ ·d ⁻¹)	1.29 ± 0.51

684 ^aResults at day seventh of the phase.

685 **Table 3.** Average of the kinetic and stoichiometric parameters obtained during growth
 686 and accumulation phase of the three cycles period.

	Growth phase					
	Cycle					
	1		2		3	
	PBR 1 & 2	PBR 3 & 4	PBR 1 & 2	PBR 3 & 4	PBR 1 & 2	PBR 3 & 4
Tested condition	25 mgN·L ⁻¹	50 mgN·L ⁻¹	35 °C	30 °C	Dark	Light
Parameter						
VSS (mg·L ⁻¹) ^a	670 ± 0.10	1,300 ± 0.14	780 ± 0.10	750 ± 0.03	697 ± 0.10	652 ± 0.10
μ (d ⁻¹) ^a	0.11	0.21	0.10	0.10	0.09	0.08
\square_{biomass} (mgVSS·L ⁻¹ ·d ⁻¹)	53.30	143.21	69.05	68.85	41.88	40.63

q_N (mgN·gVSS·d ⁻¹)	7.74	10.46	6.74	6.56	6.00	5.59
$Y_{X/N}$	14.91	20.05	14.32	14.69	14.47	15.21
Accumulation phase						
Cycle						
	1		2		3	
	PBR 1 & 2	PBR 3 & 4	PBR 1 & 2	PBR 3 & 4	PBR 1 & 2	PBR 3 & 4
Tested condition	25 mgN·L ⁻¹	50 mgN·L ⁻¹	35 °C	30 °C	Dark	Light
Parameter^a						
PHB (%dcw)	4.6 ± 2.7	1.75 ± 0.5	3.4 ± 0.42	2.3 ± 0.85	8.2 ± 6.90	0.75 ± 0.21
\square_{PHB} (mgPHB·L ⁻¹ ·d ⁻¹)	3.93 ± 2.7	1.48 ± 0.5	4.04 ± 0.42	1.51 ± 0.85	13.61 ± 6.90	0.85 ± 0.21

687 ^aResults at day seventh of the phase

688 **Table 4.** Average and standard deviations of the kinetic and stoichiometric parameters

689 obtained during growth of the 9 performed repetitions.

Growth phase		
Parameter	PBR 1	PBR 2
VSS (mg·L ⁻¹) ^a	739.78 ± 227.87	750.88 ± 226.57
μ (d ⁻¹) [*]	0.13 ± 0.04	0.12 ± 0.03
$\square_{biomass}$ (mgVSS·L ⁻¹ ·d ⁻¹)	77.78 ± 24.91	74.87 ± 18.42
q_N (mgN·gVSS·d ⁻¹)	6.61 ± 1.86	6.86 ± 2.14
$Y_{X/N}$	19.42 ± 2.37	18.45 ± 2.37

690 ^aResult at day seventh.

691

692 **Table 5.** Results on PHB production of each of the 9 performed repetitions. Values

693 were calculated at day seventh of accumulation.

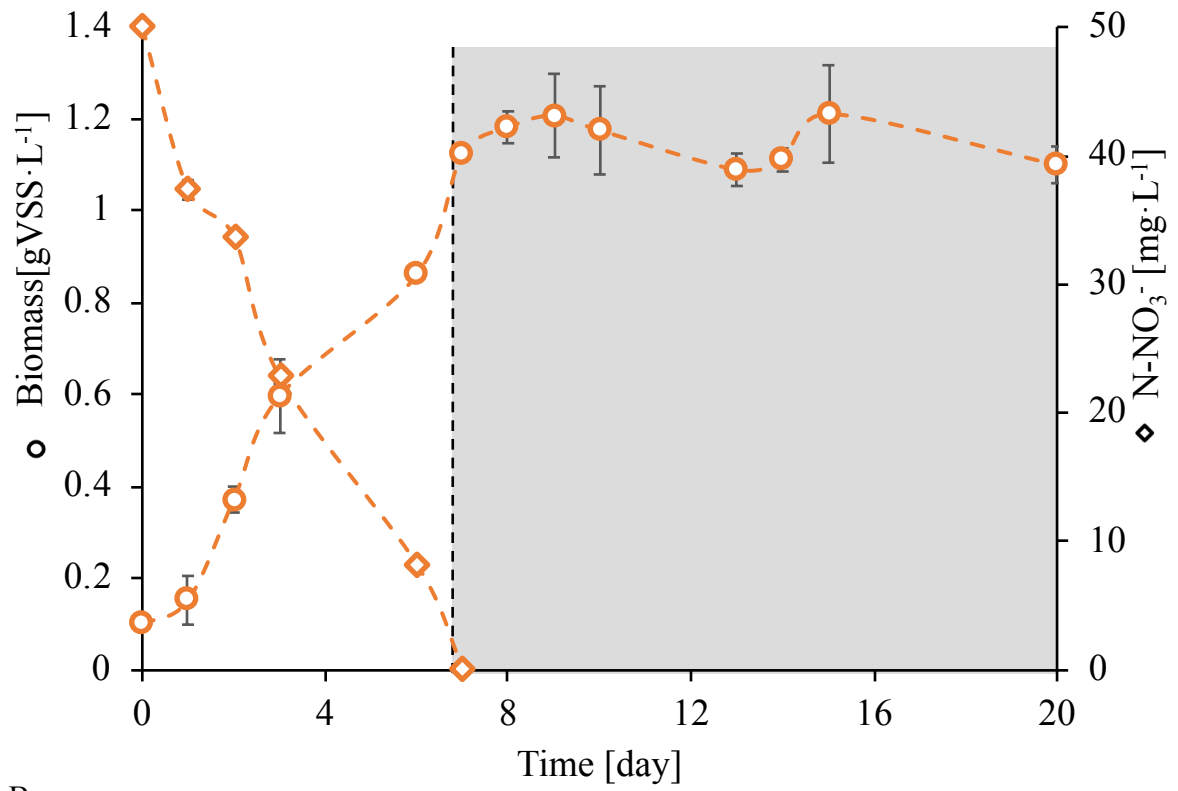
Accumulation phase						
Repetition	PHB (%dcw)		\square_{PHB} (mgPHB·L ⁻¹ ·d ⁻¹)		Y_{PHB/Ac} (g PHB_{COD}/g Ac_{COD})	
	PBR 1	PBR 2	PBR 1	PBR 2	PBR 1	PBR 2
1	2.3	3.8	3.14	5.17	0.13	0.2
2	13.4	5.2	8.99	0	0.24	0.1
3	8.8	3.3	4.65	1.46	n.d.	n.d.
4	14.9	4.4	10.18	2.72	0.27	0.09
5	10.6	5.8	11.98	9.85	0.24	0.21
6	1.8	4.6	1.93	5.96	n.d.	n.d.
7	4.6	4.6	5.74	4.38	n.d.	n.d.
8	4.2	7.7	3.64	6.24	0.12	0.36
9	1.7	21.6	0.88	9.74	0.04	0.4

694 n.d. stands for no data.

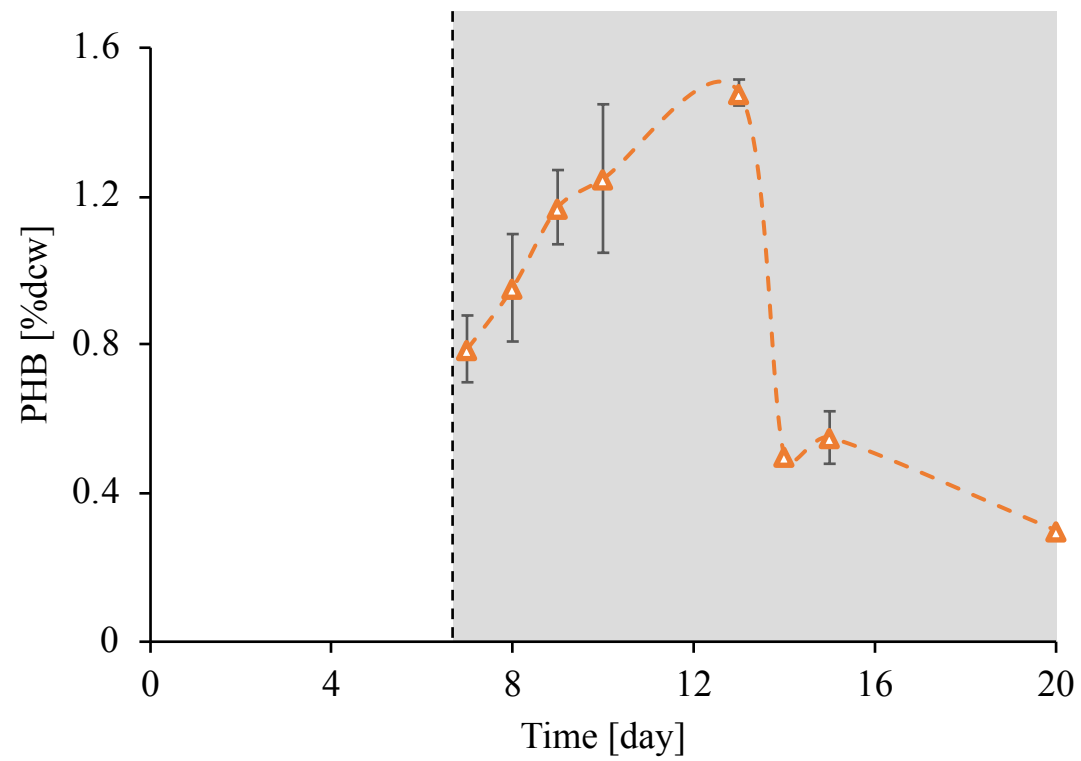
695

696

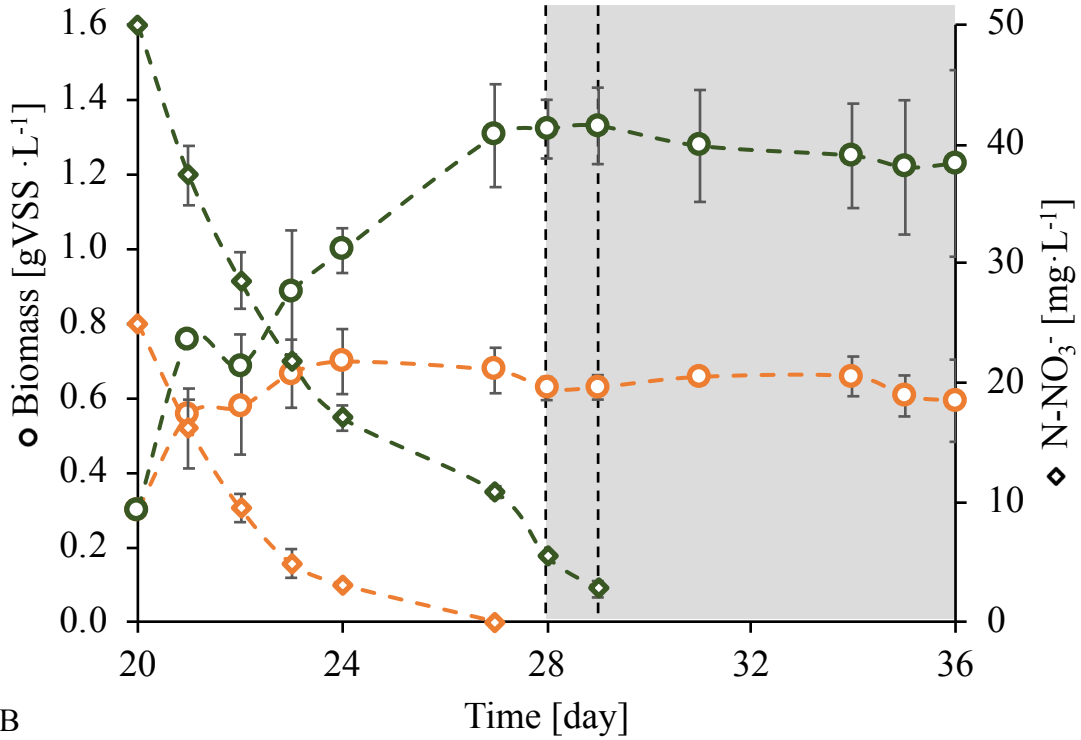
A



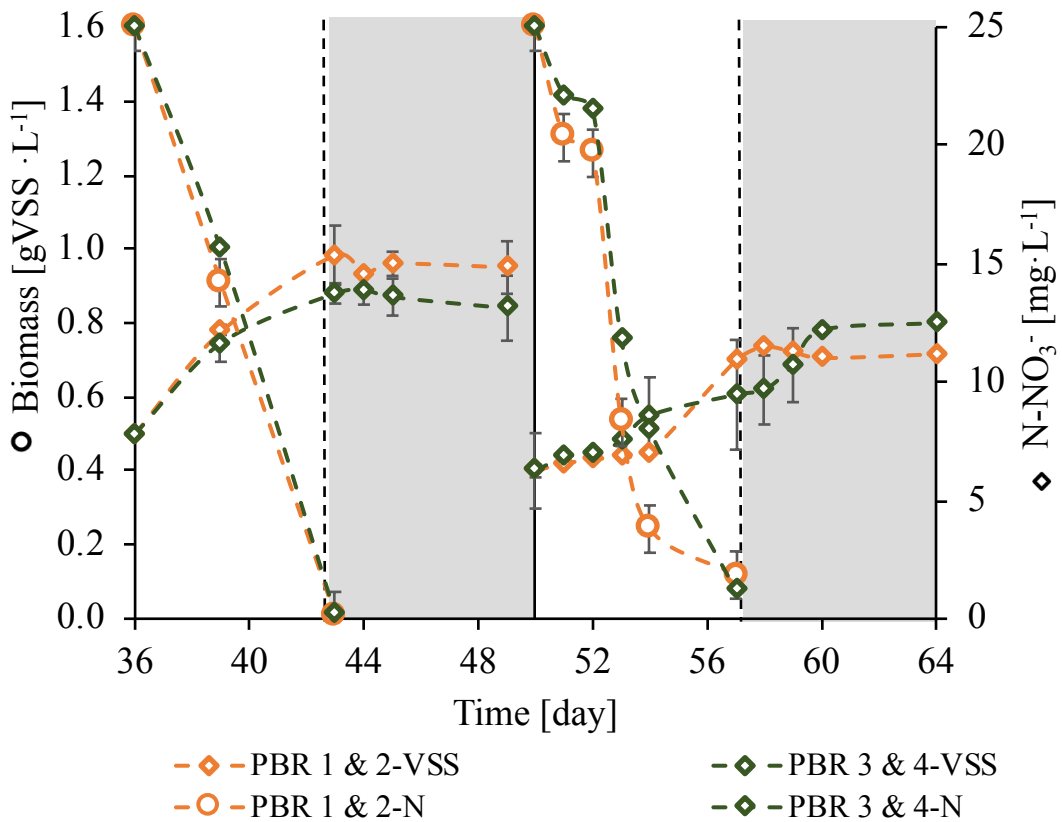
B



A



B



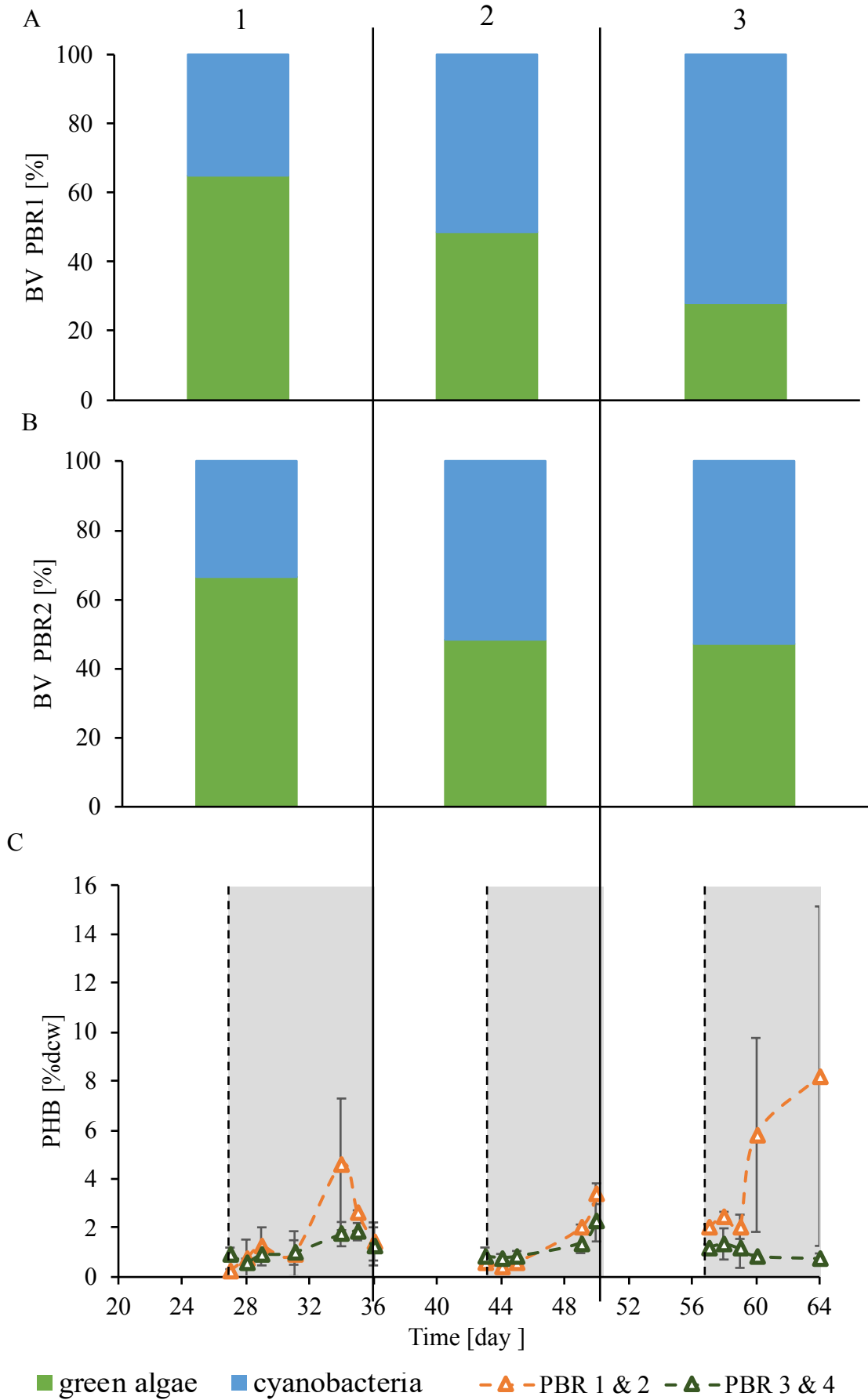
—◇— PBR 1 & 2-VSS

—○— PBR 1 & 2-N

—◇— PBR 3 & 4-VSS

—◇— PBR 3 & 4-N

Cycle



Repetition

